ChemComm

A Conformational Study of the 10-23 DNAzyme via Programmed DNA Self-Assembly

Journal:	*ChemComm*
Manuscript ID	CC-COM-02-2022-001144.R2
Article Type:	Communication

COMMUNICATION

A Conformational Study of the 10-23 DNAzyme via Programmed DNA Self-Assembly

Received 00th January 20xx,
Accepted 00th January 20xx

DOI: 10.1039/x0xx00000x

Dake Mao[a], Qian Li[a,b], Qian Li[a], Pengfei Wang[c], Chengde Mao*[a]

This communication measures the inter-helical angle of the 10-23 DNAzyme-substrate complex by atomic force microscopy (AFM). specificity. Herein, we have devised a strategy to assemble the DNAzyme-substrate complex into a periodic DNA 2D array, which allows reliable study of the conformation of the 10-23 DNAzyme by AFM imaging and fast Fourier transform (FFT). Specifically, the angle between the two flanking helical domains of the catalytic core has been determined via the repeating distance of 2D array. We expect that the same strategy can generally be applicable for studying other nucleic acid structures.

DNAzymes,[1,2] since their discovery from *in vitro* selection processes, have been explored in a wide variety of applications[3,4] including biosensors,[5-8] nanomachines,[9-12] and gene suppression.[13-15] Among them, 10-23 DNAzyme is one of the most remarkable enzymes, which can efficiently cleave RNA with sequence-specificity.[16,17] It consists of two-variable arms and a conserved, 15-base-long, catalytic core (Fig. 1a). The two arms can hybridize with RNA substrates via Watson-Click base-pairing and provide sequence specificity. It is of great interest to determine the 3D structure of the enzyme-substrate complex for understanding its catalytic mechanism. Despite extensive efforts including crystallographic study, determining its 3D structure remains a challenge. For example, in an effort of crystallographic study, the 10-23 DNAzyme and its substrate form four-strand complexes, which are not catalytically relevant.[18,19] While this manuscript was under preparation, an NMR study was reported to deduct the 10-23 DNAzyme catalytic structure.[20] Herein, we report a rapid and convenient structural study of the global conformation of the DNAzyme-substrate complex. The inter-helical angle (θ) between the two flanking duplex arms in the DNAzyme-substrate complex has been directly measured by atomic force microscopy (AFM). The same approach is expected to be applicable to determine the bend angles of other biological nucleic acids involved in various biological processes,[21,22] including transcription,[23-25] gene regulation,[26-28] and catalytic nucleic acids.[29,30]

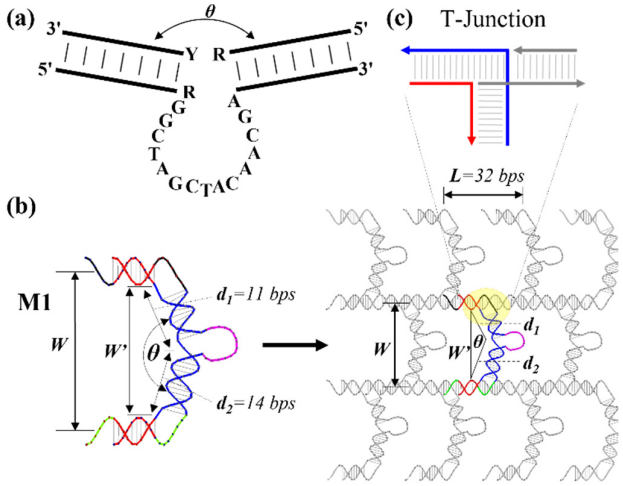

Fig. 1 Self-assembly of 10-23 DNAzyme into 2D arrays for conformational study. (a) A complex of a 10-23 DNAzyme (bottom) and its RNA substrate (top). The DNAzyme contains a 15-base-long catalytic core (sequence shown) and two recognition arms that hybridize with the RNA substrate. [R: A or G; Y: U or C]. (b) Self-assembly of a 10-23 DNAzyme-substrate complex into 2D arrays. A 10-23 DNAzyme–substrate complex (pink: catalytic core) is engineered into a two-stranded, C–shaped motif **M1**. The same coloured (green or black) tail and internal loop are complementary to each other. Their hybridization forms T-junctions, which arrange the motifs into brick-wall-like 2D arrays. (c) The detailed structure of a T-junction.

In this communication, we used atomic force microscopy (AFM) imaging to directly measure the inter-helical angle (θ) between the two flanking duplex arms in the DNAzyme-substrate complex. Since all RNA residues in the RNA substrate can be replaced by DNA residues except the RNA residue 5' to the phosphodiester bond to be cleaved for the enzyme activity, a non-cleavable DNA molecule with the same

[a] *Department of Chemistry, Purdue University, West Lafayette, IN, 47907, USA. Email: mao@purdue.edu*
[b] *College of Life Sciences, Northwest University, Xi'an, Shaanxi 710069, China.*
[c] *Institute of Molecular Medicine, Shanghai Key Laboratory for Nucleic Acid Chemistry and Nanomedicine, State Key Laboratory of Oncogenes and Related Genes, Renji Hospital, School of Medicine, Shanghai Jiao Tong University, Shanghai 200127, China.*
Electronic Supplementary Information (ESI) available: [details of any supplementary information available should be included here]. See DOI: 10.1039/x0xx00000x

sequence was used as the substrate analog to study the DNAzyme-substrate complex. The change is quite minimal (one hydroxyl group) and is unlikely to significantly impact on the complex structure. Indeed, similar modifications (changing one 2' –OH to 2' –F or–OCH_3) were been used literature and shown little impact on the complex structure.[18, 20] In principle, we could use AFM imaging to investigate the conformation of individual DNAzyme-substrate complexes. However, the conformation of the individual complex would be easily deformed during AFM sample preparation by fluidic shearing and sample-surface interactions. To overcome this problem, we applied structural DNA nanotechnology[31,32] to this study. The complex was incorporated into periodic, brick-wall-like, two-dimensional (2D) arrays as illustrated in Fig. 1. Such arrays will be resistant to structural disturbs accompanying sample handling and eliminate individual fluctuations in a similar fashion as in studies of single crystals X-ray diffractions. The building block for the arrays was a two-stranded, C-shaped motif (**M1**). It contains multiple domains: four helical domains, two internal, 6-nucleotide (nt)-long, single-stranded loops, the 10-23 DNAzyme catalytic core (pink), and two 6-nt-long, single-stranded, tails at both ends. The tail and loop with the same color are complementary to each other and their hybridization leads to the formation of a T-junction.[33-36] In the presence of Mg^{2+}, T-junctions are stable, and the DNA motifs will associate with each other to form 2D arrays. The outside, two, helical domains will form the continuous horizontal, longitude duplexes, while the central DNAzyme domain (including the catalytic core and two flanking helical domains) will form discrete, vertical, latitudinal duplexes. According to our motif design, the 2D arrays will not impose any conformational constraints onto the DNAzyme. Thus, The DNAzyme would be in the native conformation.

The interhelical angle (θ) can be determined by AFM imaging of the assembled DNA arrays. Due to the resolution limit of AFM imaging, it is impossible to accurately and directly measure the θ angle of each DNAzyme from the images.

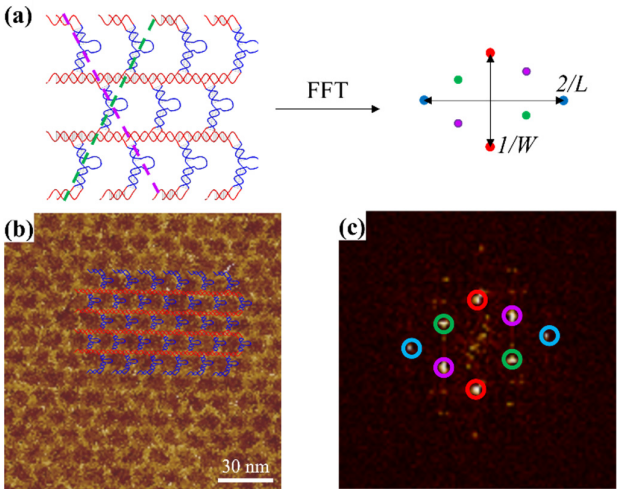

Fig. 2 FFT analysis of 2D array (a) Schematic drawing of FFT analysis, the red and blue spots matched with repeating longitudinal and latitudinal duplexes, respectively. The green and purple spots indicate the repeating feature of the green and purple dashed lines, respectively. (b) Schematic model of DNA arrays overlapped with experimental, atomic force microscopy (AFM) image. (c) FFT pattern of the AFM image (b), the circled spots are related to the schematic FFT pattern in (a) in the same color.

However, θ could be accurately calculated from measured experimental data (Fig. 2). In the 2D array, two sets of parallel lines were drawn to fit the longitude lines (red) and the latitude lines (blue). The repeating distances between the longitude lines (*W*) and between the latitude lines (*L*) were measured by fast Fourier transform (FFT). In the FFT pattern of the 2D array (Fig. 2a), the long- (blue) and the short-distanced (red) pairs of spots corresponded to the latitude (d = 0.5*L*) and longitude (d = *W*) repeating lines, respectively. Note, another pair of spots (green and purple) were also generated (corresponding to the green and purple lines, respectively) because of the periodic feature of array (Fig. 2a, green and purple lines and spots). *L* is independent of DNAzyme conformation. In the current design, it is three helical turns (32 base pairs, bps) long, or 10.56 nm long (assuming 0.33 nm/bp). For each single-crystalline, the measured value of *W* could be calibrated by the value of *L* to remove the experimental error and obtain an accurate value. To be specific, the ratio between real *L* and measured *L'* was used to calibrate the measured *W* from 2D FFT. We can further obtain the edge-to-edge distance (*W'*) between longitude DNA duplexes:

$$W' = W/L' * 10.56 \text{ nm} - 2 \text{ nm}$$

Note that the DNA duplex has a diameter of 2 nm. According to the motif design and experimental conditions, the longitude duplex will keep in B-DNA form and the diameter was considered as a constant.[37] The angle (θ) can be therefore calculated as:

$$W'^2 = d_1^2 + d_2^2 - 2d_1d_2\cos\theta$$

W can be measured from AFM images; d_1 and d_2 are designed to be 3.63 nm (11 bps) and 4.62 nm (14 bps) long, respectively.

We have followed the previously reported substrate-assisted self-assembly method to assemble the DNA 2D arrays. Briefly, the two-component strands were mixed at an equal molar ratio in an Mg^{2+}-containing, neutral, aqueous buffer with a freshly cleaved mica together and slowly cooled down from 95 °C to 4 °C over 48 hours. After assembly, the DNA samples were directly visualized by fluid-mode AFM imaging. As shown in the AFM images, brick wall-like 2D arrays were clearly visible (Fig. 2b). A section profile was plotted along the continuous duplexes of brick-like walls to determine the distance between two adjacent DNAzyme domains, which resulted in an average of 12.0 nm (Fig. S2a), agreeing well with the theoretical value (10.56 nm). The schematic model of a DNA 2D array could fit with the experimental AFM image nicely (Fig. 2b). To perform a 2D FFT, the areas of AFM images were chosen so that each area contains only one continuous single-crystalline 2D array.

Single-crystalline 2D arrays were measured to determine

Table 1 Calculated results and theoretical value

Motif	d_1 (nm)	d_2 (nm)	*L* (nm)	Theoretical θ and *W*	Measured θ or *W*
M1	3.63	4.62	10.56	N. A.	θ = 125.3 ± 27.3°
M2	4.29	4.29	10.56	θ_D = 180°	
				W_D = 8.58 nm	W_D = 8.53 ± 1.37 nm
M3	4.29	4.29	10.56		
				θ_H = 120°	θ_H = 130.5 ± 19.0°

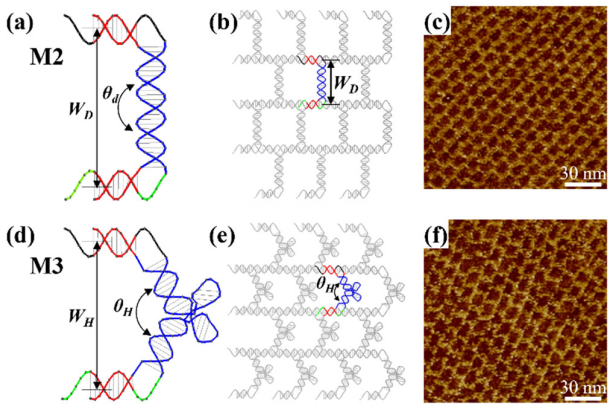

Fig. 3 Self-assembly of control DNA structures. (a-c) The 2D array incorporated with a DNA duplex. (d-f) The 2D array incorporated with a Holliday junction. (a and d) Motifs design. (b and e) Scheme of assembled 2D arrays. (c and f) Corresponding AFM images.

the angle (θ) between the two flanking duplexes of the DNAzyme-substrate complex (Fig. S4, Tab. S1). From the experimentally measured *W*′ value, we calculated the angle θ among each chosen array. Its value varies from 78° to 164° and fits with the Gaussian distribution (Fig. S3a), suggesting that the inter-duplex angle θ is considerably flexible. The average value and standard deviation were calculated as 125.3 ± 27.3° (Table 1).

To validate this method, we applied it to two known DNA structures (Fig. 3): a simple duplex (θ_d: 180°, Fig. 3a-3c) and a Holliday junction (θ_H: 120°, Fig. 3d-3e).[37-39] Correspondingly, two new C-shaped motifs were designed, in which, the vertical DNAzyme domain was replaced by a 26-bp duplex (in **M2**) or a Holliday junction domain (in **M3**). The 2D arrays were assembled and measured in the same way as for arrays of **M1** (containing the 10-23 DNAzyme). Section analysis was performed for **M2** and **M3** array to determine the repeating distances between the latitude features, and the results agreed with theoretical values (Fig. S2b, S2c). For **M2**, 20 single-crystalline 2D arrays were measured (Fig. S5, Tab. S2). The W_D was measured to be 8.53 ± 1.37 nm, matching the theoretical length 8.84 nm of a 26-bp duplex (Fig. S3b, Table 1), indicating the value of θ_d is 180°. For **M3**, 11 single-crystalline 2D arrays were measured (Fig. S6, Tab. S3) and the deduced angle θ_H: 130.5 ± 19.0°, consistent with the value (120°) reported before (Fig. S3c, Table 1).[37,38] The preserved angle of Holliday junction indicates that our DNA 2D array design doesn't impose structural strain to target DNA secondary structure. For these two known structures, the values measured from this AFM-based method are consistent with the values reported before. Thus, this method is valid. Furthermore, these control experiments demonstrated that this strategy is a general-applicable approach.

In summary, we applied the principle of structural DNA nanotechnology to study the conformation of the 10-23 DNAzyme-substrate complex, specifically, measured the inter-duplex angle (θ) in the complex. At the final stage of the preparation of this manuscript, we became aware of a recent NMR study of 10-23 DNAzyme.[20] The measured interhelical angle (122°, supplementary information and Fig. S7) is well consistent with our measurement. This work demonstrates that programmed self-assembly can be used in biophysical studies of other biomacromolecules. It complements other biophysical techniques such as fluorescence resonant energy transfer (FRET),[40] NMR,[41] and X-ray crystallography.[42,43] However, it doesn't require labeling or growing high-quality crystals or complicated data interpretation in NMR. We expect that this approach would greatly facilitate the structural study of biomacromolecules, particularly those about DNAs and RNAs.

This work was supported by the NSF (2025187 and 2107393 to C.M.) and NSFC (22074118 to Q.L.).

Conflicts of interest

There are no conflicts to declare.

Notes and references

1 R. R. Breaker and G. F. Joyce, *Chem. Biol.*, 1994, **1**, 223–229.
2 B. Cuenoud and J. W. Szostak, *Nature*, 1995, **375**, 611–614.
3 I. Willner, B. Shlyahovsky, M. Zayats and B. Willner, *Chem. Soc. Rev.*, 2008, **37**, 1153–1165.
4 L. Ma and J. Liu, *iScience*, 2020, **23**, 100815.
5 J. Li and Y. Lu, *J. Am. Chem. Soc.*, 2000, **122**, 10466–10467.
6 J. Liu and Y. Lu, *J. Am. Chem. Soc.*, 2003, **125**, 6642–6643.
7 L. M. Lu, X. B. Zhang, R. M. Kong, B. Yang and W. Tan, *J. Am. Chem. Soc.*, 2011, **133**, 11686–11691.
8 F. Wang, J. Elbaz, C. Teller and I. Willner, *Angew. Chem. Int. Ed.*, 2011, **123**, 295–299.
9 Y. Chen, M. Wang and C. Mao, *Angew. Chem. Int. Ed.,* 2004, **116**, 3554–3557.
10 Y. Tian, Y. He, Y. Chen, P. Yin and C. Mao, *Angew. Chem. Int. Ed*, 2005, **117**, 4355–4358.
11 T. G. Cha, J. Pan, H. Chen, J. Salgado, X. Li, C. Mao and J. H. Choi, *Nat. Nanotechnol.*, 2014, **9**, 39–43.
12 J. Wang, L. Yue, Z. Li, J. Zhang, H. Tian and I. Willner, *Nat. Commun.*, 2019, **10**, 4963.
13 M. Cieslak, J. Niewiarowska, M. Nawrot, M. Koziolkiewicz, W. J. Stec and C. S. Cierniewski, *J. Biol. Chem.*, 2002, **277**, 6779–6787.
14 L. Zhang, W. J. Gasper, S. A. Stass, O. B. Ioffe, M. A. Davis and A. J. Mixson, *Cancer Res.*, 2002, **62**, 5463–5469.
15 H. Fan, Z. Zhao, G. Yan, X. Zhang, C. Yang, H. Meng, Z. Chen, H. Liu and W. Tan, *Angew. Chem. Int. Ed.*, 2015, **54**, 4801–4805.
16 S. W. Santoro and G. F. Joyce, *Proc. Natl. Acad. Sci. U. S. A.*, 1997, **94**, 4262–4266.
17 S. W. Santoro and G. F. Joyce, *Biochemistry*, 1998, **37**, 13330–13342.
18 J. Nowakowski, P. J. Shim, G. S. Prasad, C. D. Stout and G. F. Joyce, *Nat. Struct. Biol.*, 1999, 6, 151–156.
19 J. Nowakowski, P. J. Shim, C. D. Stout and G. F. Joyce, *J. Mol. Biol.*, 2000, **300**, 93–102.
20 J. Borggräfe, J. Victor, H. Rosenbach, A. Viegas, C. G. W. Gertzen, C. Wuebben, H. Kovacs, M. Gopalswamy, D. Riesner, G. Steger, O. Schiemann, H. Gohlke, I. Span and M. Etzkorn, *Nature,* 2022, **601**, 144–149.
21 S. Harteis and S. Schneider, *Int. J. Mol. Sci.*, 2014, **15**, 12335–12363.

22 M. H. Werner, A. M. Gronenborn, G. M. Clore, M. H. Werner, A. M. Gronenborn and G. M. Clore, *Science*, 1996, **271**, 778–784.
23 J. M. Passner and T. A. Steitz, *Proc. Natl. Acad. Sci. U. S. A.*, 1997, **94**, 2843–2847.
24 A. A. Napoli, C. L. Lawson, R. H. Ebright and H. M. Berman, *J. Mol. Biol.*, 2006, **357**, 173–183.
25 J. J. Love, X. Li, D. A. Case, K. Gieset, R. Grosschedlt and P. E. Wright, *Nature*, 1995, **376**, 791–795.
26 I. Querques, M. Schmitz, S. Oberli, C. Chanez and M. Jinek, *Nature*, 2021, **599**, 497–502.
27 C. Hu, C. Almendros, K. H. Nam, A. R. Costa, J. N. A. Vink, A. C. Haagsma, S. R. Bagde, S. J. J. Brouns and A. Ke, *Nature*, 2021, **598**, 515–520.
28 J. Romanuka, G. E. Folkers, N. Biris, E. Tishchenko, H. Wienk, A. M. J. J. Bonvin, R. Kaptein and R. Boelens, *J. Mol. Biol.*, 2009, **390**, 478–489.
29 E. A. Doherty and J. A. Doudna, *Annu. Rev. Biochem.*, 2000, **69**, 597–615.
30 P. H. Aniela Wochner, James Attwater and Alan Coulson, *Science*, 2011, **332**, 209–212.
31 N. C. Seeman, *J. Theor. Biol.*, 1982, **99**, 237–247.
32 N. C. Seeman, *Nature*, 2003, **421**, 427–431.
33 S. Hamada and S. Murata, *Angew. Chem. Int. Ed.*, 2009, **121**, 6820–6823.
34 X. Li, C. Zhang, C. Hao, C. Tian, G. Wang and C. Mao, *ACS Nano*, 2012, **6**, 5138–5142.
35 C. Tian, C. Zhang, X. Li, C. Hao, S. Ye and C. Mao, *Langmuir*, 2014, **30**, 5859–5862.
36 Q. Li, L. Liu, D. Mao, Y. Yu, W. Li, X. Zhao and C. Mao, *J. Am. Chem. Soc.*, 2020, **142**, 665–668.
37 A. Travers and G. Muskhelishvili, *FEBS J.*, 2015, **282**, 2279–2295.
38 C. Mao, W. Sun and N. C. Seeman, *J. Am. Chem. Soc.*, 1999, **121**, 5437–5443.
39 R. Sha, F. Liu, D. P. Millar and N. C. Seeman, *Chem. Biol.*, 2000, **7**, 743–751.
40 R. Sha, F. Liu and N. C. Seeman, *Biochemistry*, 2002, **41**, 5950–5955.
41 E. A. Jares-Erijman and T. M. Jovin, *Nat. Biotechnol.*, 2003, 21, 1387–1395.
42 S. S. Wijmenga and B. N. M. Van Buuren, *Prog. Nucl. Magn. Reson. Spectrosc.*, 1998, **32**, 287–387.
43 A. T Brünger, *Nat. Struct. Biol.*, 1997, **4** (suppl.), 862–865.
44 H. Liu, X. Yu, Y. Chen, J. Zhang, B. Wu, L. Zheng, P. Haruehanroengra, R. Wang, S. Li, J. Lin, J. Li, J. Sheng, Z. Huang, J. Ma and J. Gan, *Nat. Commun.*, 2017, **8**, 2006.